Long-Range Correlations in a Polymer Chain Due to Its Connectivity

David Shirvanyants,[†] Sergey Panyukov,[‡] Qi Liao,[§] and Michael Rubinstein*,[†]

Department of Chemistry, University of North Carolina at Chapel Hill, North Carolina 27599-3290, P. N. Lebedev Physics Institute, Russian Academy of Sciences, Moscow 117924, Russia, and State Key Laboratory of Polymer Physics and Chemistry, Joint Laboratory of Polymer Science and Materials, Institute of Chemistry, Chinese Academy of Sciences, Beijing 100080, China

Received June 29, 2007; Revised Manuscript Received November 29, 2007

ABSTRACT: The analysis of intrachain monomeric interactions reveals a new effect in the description of polymer conformations in dilute θ-solutions, semidilute solutions, and melts. The chain connectivity modifies the effective monomeric interaction, which results in the long range correlations between orientations of polymer bonds, that decay as a power law. A major modification of the standard polymer models was made to describe this effect. We predict the power-law decay of the bond-vector correlation function of a polymer in the θ-solvent, $\langle \mathbf{a}_i \mathbf{a}_j \rangle \sim |i - j|^{-3/2}$, ($\mathbf{a}_i$ is the ith bond vector) instead of commonly assumed exponential decay. We calculated the length dependence of the ratio of the mean squared size of a chain segment to its length s. Our theory predicts that this ratio has a maximum below the θ-point due to the balance of the new effective interaction and the two-body attraction. The Flory characteristic ratio C_n of a chain with n main chain bonds is found to approach its asymptotic value C_∞ as $n^{-1/2}$ and not as n^{-1}, predicted by the classical polymer models. We show that the necessary conditions for the existence of new effective interactions is the chain connectivity and nonzero range of monomeric interactions.

1. Introduction

Polymer chains have different conformations depending on interactions between their monomers. If interactions are predominately repulsive, as in the case of good solvent solutions, polymers swell, while if their interactions are attractive, as in the case of a poor solvent, chains are collapsed. Between these two cases there is a special condition, called θ-point, under which the effective interaction between monomers is zero and the chain is almost ideal. Similar compensation of attractive and repulsive parts of monomeric interactions occurs in polymer melts and concentrated solutions. In semidilute solutions the effective interactions vanish on length scales larger than the correlation length ξ due to the screening of the excluded volume by surrounding chains. Polymers with vanishing effective interactions, such as in θ-solvents and melts, are traditionally described by the ideal chain models.[1–12]

In an ideal chain there are no interactions between monomers that are far apart along the polymer. Interactions of neighboring monomers along the polymer (due to chain stiffness or local steric hindrance) lead to exponentially decaying correlations in directions of vectors $\mathbf{a}_i$ and $\mathbf{a}_j$ of bonds i and j separated by the distance $s = a|i - j|$ along the chain

$$h(s) \equiv \langle \mathbf{a}_i \mathbf{a}_j \rangle / a^2 \sim e^{-s/l_p} \qquad (1)$$

where a is the bond length and l_p is the persistence length. Rapid decay of bond vector correlations results in the random walk statistics of the chain on curvilinear length scales larger than the persistence segment length l_p. The concept of the persistence length is widely used for the characterization of the polymer flexibility.[13–17] Polymers with persistence length, l_p, on the order of several bond lengths, a, are called flexible, while chains with $l_p \gg a$ are called semiflexible. Single stranded DNA ($l_p \approx 2$

nm) is an example of a flexible chain, while double strained DNA ($l_p \approx 50$ nm) is a common example of a semiflexible polymer.

The assumption of ideality of chains in melts and concentrated solutions was recently demonstrated to be incorrect.[18] Using both computer simulations and theoretical estimates it was shown that bond vector correlation function $h(s)$ in melts and semidilute solutions decays as the power law of the curvilinear distance s between bonds

$$h(s) \sim s^{-3/2} \qquad (2)$$

This unexpectedly slow decay of correlations was explained by the effect of the correlation hole,[19] leading to relative compression of the chain with respect to its ideal state.

Notice that the correlation hole effect is the prominent feature of melts or concentrated solutions of polymer chains and is absent for chains in dilute θ-solutions. Since the interaction between monomers at the θ-point is compensated by their interaction with molecules of the solvent, one can naively expect to observe ideal-like behavior of such chains. In this paper we demonstrate that polymers in dilute θ-solutions are not ideal and exhibit the same power law decay of the bond correlation function (eq 2). We will show that the ideal chain behavior at the θ-point is destroyed due to the connectivity induced effective interaction between monomers that are far away from each other along the chain. Such monomers do interact when they approach each other in space, but the contributions of attractive and repulsive parts of the interaction to the effective second virial coefficient compensate each other at the theta point. The main result of this paper is that connectivity of chain monomers leads to additional correlations in their relative position in space causing incomplete compensation of attractive and repulsive interactions at the θ-point. The connectivity of monomers in the chain slightly decreases the probability of the two monomers to be within the range of the attractive well of the interaction potential. The magnitude of this effect depends on the distance between the two monomers along the chain contour. This

[†] Department of Chemistry, University of North Carolina at Chapel Hill.
[‡] P. N. Lebedev Physics Institute, Russian Academy of Sciences.
[§] State Key Laboratory of Polymer Physics and Chemistry, Joint Laboratory of Polymer Science and Materials, Institute of Chemistry, Chinese Academy of Sciences.

probability shift leads to an additional effective interaction of two monomers belonging to the same chain.

Another manifestation of the probability shift is the presence at θ-conditions of the large correction term $\sim\sqrt{n}$ to the expected dependence $R^2 \sim n$ of the mean square size R^2 of the polymer chain on the number n of its main chain bonds. This change of the polymer size can be observed experimentally by measuring the dependence of the Flory characteristic ratio C_n on the number of chain bonds n.

We will show that this new connectivity-induced interaction results in the power law decay of the bond vector correlation function (eq 2) for all quasi-ideal chains, including polymers in θ-solvents, melts, and concentrated solutions. This interaction was not taken into account in the classical polymer models.

It is well-known that three (and higher) body interactions shift the effective θ-temperature relative to the Flory's θ-temperature of the "gas of unconnected monomers".[21] In addition to the shifted θ-point these many-body interactions lead to logarithmic corrections to the chain size in the tricritical region.[11,12,20] We show that the power law dependence (eq 2) with similar logarithmic corrections (which are important only for very long chains) is the dominant effect in the significant temperature range near the shifted θ-temperature.

In this paper, we discuss the origin and consequences of the new connectivity-induced correlation effect. Analytical theory of connectivity-induced correlations is proposed in sections 2.1–2.3 and its predictions are compared with the results of computer simulations in section 2.4. In section 2.5, we take into account the chain flexibility in our new theory and demonstrate that our theory is in excellent agreement with numerical data. The importance of the connectivity-induced interactions for the dependence of the chain section size on the number of monomers in this section and the temperature is demonstrated in section 3.1. In section 3.2, we calculate the molecular weight dependence of the Flory characteristic ratio at θ-conditions and show that it is in good agreement with experiments. The main predictions of our new model of the connectivity-induced long range correlations in polymers are summarized in section 4.

2. Bond Vector Correlation Function

2.1. Telechelic Model. In the ideal chain model there are no long range correlations between orientations of bonds along the chain. Such correlations appear as a result of interactions between chain monomers. In order to study the effect of interactions on bond orientations we first consider the telechelic model of a Gaussian chain (see Figure 1) consisting of $n + 1$ monomers, with only two end monomers interacting with each other via a short-range potential $U(r)$, which depends on the length of the end-to-end vector $\mathbf{r}$ of the chain

$$\mathbf{r} = \sum_{i=1}^{n} \mathbf{a}_i \tag{3}$$

Here $\mathbf{a}_i$ is the ith bond vector with an average length a. This model will be generalized in section 2.2 in order to take into account interactions between all monomers of the real chain.

The correlation function of bond vectors i and j of the telechelic chain with contour length $L = an$

$$H(L) \equiv \langle \mathbf{a}_i \mathbf{a}_j \rangle / a^2 \tag{4}$$

does not depend on their positions along the chain contour, nor on the distance along the chain $s = a|i - j|$ between them, since the probability of a chain conformation is proportional to its
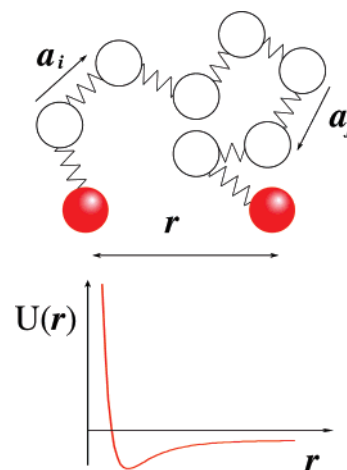

Figure 1. In a telechelic chain, only two monomers are interacting with each other with the potential $U(r)$ sketched in the lower part of the figure, while other monomers do not interact at all.

Boltzmann weight, which depends in this model only on the sum of all bond vectors $\mathbf{a}_i$, that is, on the end-to-end vector $\mathbf{r}$, eq 3. The correlation function $H(L)$ is calculated in two steps:

First, the scalar product $\mathbf{a}_i \mathbf{a}_j$ is averaged over all fluctuations of bond vectors for given value r of the end-to-end vector $\mathbf{r}$ (see Appendix A for details)

$$H(L|r) \equiv \langle \mathbf{a}_i \mathbf{a}_j \rangle_r / a^2 = (r^2 - aL)/L^2 \tag{5}$$

According to this expression the two bond vectors are not correlated only if r is equal to the root-mean-square end-to-end distance of the chain, $\sqrt{aL}$. They have the same preferential orientation (along the end-to-end vector $\mathbf{r}$, with $H(L|r) > 0$) for stretched chain, $r^2 > aL$, and opposite preferential orientation (with $H(L|r) < 0$) if the chain is compressed, $r^2 < aL$.

Second, we calculate $H(L)$, eq 4, averaging the result of the first step, $H(L|r)$ (see eq 5), over different end-to-end distances r with the Boltzmann weight, $\sim e^{-U(r)/k_B T}$, determined by the potential $U(r)$ between two interacting monomers (see Appendix B):

$$H(L) = \frac{1}{a^2} \langle \mathbf{a}_i \mathbf{a}_j \rangle = \left(\frac{3}{2\pi}\right)^{3/2} \left(\frac{B}{a^{1/2} L^{5/2}} + \frac{5}{2} \frac{A}{a^{3/2} L^{7/2}} + ...\right) \tag{6}$$

Here B is the second virial coefficient

$$B = -\int f(r) \, \mathrm{d}^3 r \tag{7}$$

with the Mayer function

$$f(r) = \mathrm{e}^{-U(r)/k_B T} - 1 \tag{8}$$

and the coefficient A in eq 6 is defined by the expression

$$A = \int f(r) r^2 \, \mathrm{d}^3 r \tag{9}$$

Note that, as expected, the bond vector correlation function does not depend on the location of bonds i and j along this telechelic chain nor on their separation $s = a|j - i|$ along the chain (the number of bonds $|j - i|$ between them), but it depends only on the contour length L between two interacting monomers of the chain.

The most important conclusion from this simple model is that at the θ-point (with zero second virial coefficient $B = 0$) correlations between bond vectors of a telechelic chain decay as a power of the curvilinear distance L along the polymer

contour between two interacting monomers $\langle \mathbf{a}_i \mathbf{a}_j \rangle \sim AL^{-7/2}$. In classical theories of the telechelic chain the bond vector correlation function $H(L)$ has only the first $\sim B$ term in eq 6, and therefore, in contrast to our new model, these theories predict the absence of the long range correlations between orientations of bonds in θ-solutions.

2.2. Polymer with All Interacting Monomers. A more realistic description of a polymer is the chain with all $n + 1$ monomers interacting with each other. The bond vector correlation function

$$h(i, j) = \langle \mathbf{a}_i \mathbf{a}_j \rangle / a^2 \tag{10}$$

of two bonds, separated by the distance $s = a|j - i|$ along the chain can be found by taking the sum of contributions of all loops which contain bond vectors $\mathbf{a}_i$ and $\mathbf{a}_j$, and formed by pairs k and m of interacting monomers with $k < i < j < m$:

$$h(i, j) = \sum_{k=1}^{i-1} \sum_{m=j+1}^{n} H[a(m - k)] \tag{11}$$

Substituting the function $H(L)$ from eq 6 and replacing the summation over indexes k and m in eq 11 by the integration over contour lengths s_k and s_m, we obtain

$$h(i, j) \simeq \left(\frac{3}{2\pi}\right)^{3/2}\left[\frac{B}{a^{5/2}} g_{1/2}(i, j) + \frac{5}{2}\frac{A}{a^{7/2}} g_{3/2}(i, j) + ...\right] \tag{12}$$

where

$$g_p(i, j) \equiv \int_0^{s_i} \mathrm{d}s_k \int_{s_j}^{L} \frac{\mathrm{d}s_m}{(s_m - s_k)^{p+2}} =$$
$$\frac{1}{p(p+1)}\left[\frac{1}{(s_j - s_i)^p} - \frac{1}{s_j^p} - \frac{1}{(L - s_i)^p} + \frac{1}{L^p}\right] \tag{13}$$

and $L = an$ is the contour length of the chain. We see, that bond vector correlations decay as a power law of the distance $s = s_j - s_i = a(j - i)$ along the chain between bonds i and j. For internal bonds of the sufficiently long chain (that is, when $1 \ll i < j \ll n$) the bond vector correlation function in the θ-region becomes

$$h(i, j) \equiv \frac{1}{a^2}\langle \mathbf{a}_i \mathbf{a}_j \rangle =$$
$$h(s) \simeq \left(\frac{3}{2\pi}\right)^{3/2}\frac{1}{a^2}\left[\frac{4}{3}\frac{B}{(as)^{1/2}} + \frac{2}{3}\frac{A}{(as)^{3/2}} + ...\right] \tag{14}$$

The second virial coefficient $B = 0$ at the θ-point, and eq 14 predicts the power law decay of the correlation function with the exponent $p = 3/2$

$$h(s) \sim s^{-3/2} \quad (\theta\text{-solvent}) \tag{15a}$$

(as long as $A \neq 0$). In the θ-region away from the θ-point the first term $\sim B$ in eq 14 dominates over the second term $\sim A$, leading to the decay of the bond vector correlation function of internal monomers with the exponent $p = 1/2$:

$$h(s) \sim s^{-1/2} \quad (A/(as) < |B| < a^{7/2}s^{-1/2}) \tag{15b}$$

The bond vector correlation function with one of the bonds at the chain end (with $i = 1$) decays at the θ-point faster than the correlation function between internal bonds, eq 15a:

$$h(1, j) \sim (s_j - a)^{-3/2} - s_j^{-3/2} \sim s_j^{-5/2}$$
$$(\text{end monomer, } \theta\text{-solvent})$$

If both bonds are at the opposite chain ends we recover eq 6 for the telechelic chain at the θ-point, $h(1, n) \sim L^{-7/2}$.

Note that it is impossible to achieve both $B = 0$ and $A = 0$ in eq 12 by varying the temperature, except for a special form of the potential U. One can design the potential with Lennard-Jones-like asymptotic behavior ($U(r) \sim r^{-6}$ at $r \rightarrow \infty$), but with damped oscillations:

$$U(r) = k_B T \ln\left\{1 + \frac{\epsilon}{k_B T}\frac{5 - 10(r/d)^2 + (r/d)^4}{[1 + (r/d)^2]^5}\right\} \tag{16}$$

where ϵ is a positive interaction parameter and d is the interaction radius. Although for this potential $A = B = 0$, the higher order terms in expansion 14 would still be nonzero, leading to the power law decay $h(s) \sim s^{-2}$ with the exponent higher than in eqs 15a and 15b.

2.3. Bond Vector Correlation Function of Flexible Chains. The above results were derived assuming that bond length a is equal to the Kuhn length b. The predictions of this model can be generalized to flexible chains with the Kuhn length on the order of several bond length. In particular, the bond vector correlation function for internal bonds, separated by the curvilinear distance $a(j - i)$, eq 14, can be rewritten for flexible chains by replacing a for b inside the bracket in eq 14:

$$h(s) \equiv \frac{1}{a^2}\langle \mathbf{a}_i \mathbf{a}_j \rangle \simeq \left(\frac{3}{2\pi}\right)^{3/2}\frac{1}{a^2}\left[\frac{4}{3}\frac{B}{(bs)^{1/2}} + \frac{2}{3}\frac{A}{(bs)^{3/2}} + ...\right]$$
$$= \tilde{A}(a/s)^{3/2} + \tilde{B}(a/s)^{1/2} + ... \tag{17}$$

where we introduced dimensionless parameters

$$\tilde{A} = \frac{2}{3}\left(\frac{3}{2\pi}\right)^{3/2}\frac{A}{a^{7/2}b^{3/2}}, \tilde{B} = \frac{4}{3}\left(\frac{3}{2\pi}\right)^{3/2}\frac{B}{a^{5/2}b^{1/2}} \tag{18}$$

Note that the bond-vector correlation function at the θ-point, eq 17 with $B = 0$, is proportional to the probability of forming a loop, consisting of s monomers

$$h(s) = \frac{1}{a^2}\frac{2A}{3} Q(s|0) \tag{19}$$

where the probability distribution $Q(s|r)$ to find ends of Gaussian chain at the given distance r is defined in eq 60 of Appendix B.

It is important to stress, that eq 17, as well as all of the analysis of the present paper, is only valid in the so-called θ-region near the θ-temperature, where the energy $k_B T|z|$ of the excluded volume interactions of the strand containing s/a bonds is less than the thermal energy $k_B T$. Here z is the interaction parameter of the strand

$$z = \left(\frac{3}{2\pi}\right)^{3/2} B \frac{(s/a)^2}{(bs)^{3/2}} \tag{20}$$

The condition $|z| \ll 1$ is always fulfilled in the region

$$|B| \ll A/(bs) \tag{21}$$

where the connectivity-induced correlation term $\sim A$ is stronger than the excluded volume contribution $\sim B$ to the bond vector correlation function in eq 17.

In addition to pairwise, there are three and higher order interactions of chain monomers, leading to two classes of renormalization of the effective pairwise interactions. The first class takes into account interactions of several neighboring monomers along the chain and results in the shift of the second virial coefficient B and the renormalization of the Kuhn length b. The condition $B = 0$ for the renormalized second virial coefficient determines the shifted θ-temperature. Below we will use notations B, b, and θ for these renormalized quantities instead of their bare values.

The second class of renormalization is related to many-body interactions of monomers separated by many bonds along the chain that can approach each other in space in the process of thermal fluctuations. It is well-known,[12] that such tricritical fluctuations renormalize the second B and the third C monomeric virial coefficients

$$B \rightarrow Bw^{-4/11} \quad C \rightarrow C/w \tag{22}$$

where the function $w = w(s)$ logarithmically increases with the length s of the chain section between interacting monomers:

$$w(s) = 1 + \frac{11C}{2\pi^2(ab)^3} \ln \frac{s}{a} \tag{23}$$

It is shown in Appendix C that such interactions also lead to the renormalization of the parameter A in eq 17:

$$A \rightarrow Aw^{-4/33} \tag{24}$$

In order for this renormalization to be important, it has to decrease the second virial coefficient B by at least the factor of 2, which occurs at the value of the parameter $w = 2^{11/4}$ (see eq 22). For a typical value of the third virial coefficient $C \simeq a^6$ and $b > a$ this renormalization can only be important for chain sections consisting of more than $s_{ren}/a \simeq \exp[(2^{11/4} - 1)2\pi^2/11] \simeq 3 \times 10^4$ bonds (see eq 23). For chain sections shorter than s_{ren} one can ignore such renormalization due to tricritical fluctuations, while for very long chains with $s > s_{ren}$ the bond vector correlation function is expected to have weak logarithmic corrections to the power law dependence on the section length s (eq 17 with A and B given by eqs 24 and 22).

2.4. Computer Simulations. To verify our analytical predictions by computer simulations, we employ the coarse-grained continuum bead–spring model of a polymer chain. A polymer in this model consists of $n + 1$ soft-sphere monomers, interacting with each other via the truncated and shifted Lennard-Jones (LJ) potential

$$U_{LJ}(r) = \begin{cases} 4\epsilon[(\sigma/r)^{12} - (\sigma/r)^6 - (\sigma/r_c)^{12} + (\sigma/r_c)^6] & r < r_c \\ 0 & r > r_c \end{cases} \tag{25}$$

where σ is the effective diameter of the bead, r is the distance between monomers, and r_c is the cutoff radius (we use $r_c = 2.5\sigma$ for all simulations). Chain connectivity is modeled by the finitely extensible nonlinear elastic (FENE) interaction potential between adjacent monomers (in addition to the LJ potential, eq 25)

$$U_{FENE}(r) = -\frac{1}{2} k_{FENE} R_0^2 \ln (1 - r^2/R_0^2) \tag{26}$$

where k_{FENE} is the spring constant and R_0 is the maximum extension of the bond, at which the interaction energy becomes infinite. In this work we choose $R_0 = 2\sigma$ and $k_{FENE} = 10\epsilon/\sigma^2$,
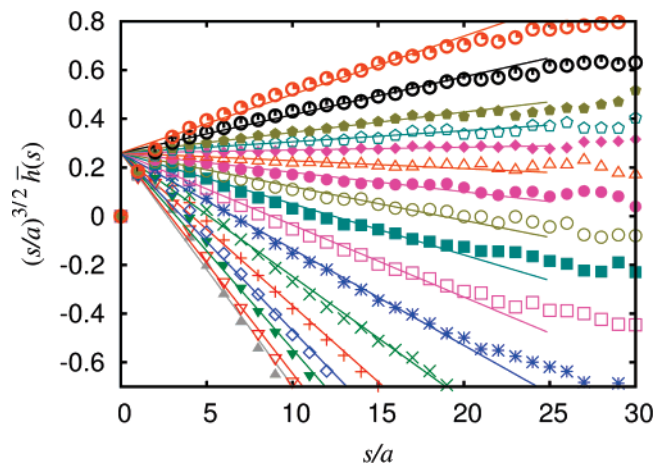
Figure 2. Dependence of the average bond vector correlation function, eq 27, multiplied by the $^3/_2$ power of the number $k = s/a$ of monomers between bonds on s/a at different temperatures. Lines are linear fits (eq 28) of the data for $5 \leq k \leq 25$. The temperatures are increasing from lower to upper curve as 1.6, 1.8, 2.0, 2.1, 2.2, 2.3, 2.4, 2.5, 2.6, 2.7, 2.8, 2.9, 3.0, 3.1, 3.2, 3.5, and 4.0 in units of ϵ/k_B.

which minimizes the n dependence of the θ-temperature.[24] New conformations are generated using the standard method of constant temperature (*NVT* ensemble) molecular dynamics. Initial configurations were created as random self-avoiding walks, and then equilibrated for at least $10\tau_R$, where τ_R is the longest relaxation time, determined from the decay of the chain end-to-end distance autocorrelation function. The resulting average length of the bond is a weak function of the temperature $a(T) = (1.03 + 0.036k_B T/\epsilon)\sigma$ in the temperature range $2\epsilon/k_B < T < 4\epsilon/k_B$.

In Figure 2, we present the bond vector correlation function

$$\bar{h}(s) \equiv \frac{1}{a^2}\overline{\langle \mathbf{a}_i \mathbf{a}_{i+k} \rangle} = \frac{1}{n-k}\sum_{i=1}^{n-k} h(i, i+k) \tag{27}$$

averaged over all pairs of monomers separated by segments of length $s = ak$ and multiplied by the number of monomers, k, between the two bonds, to the power 3/2. Since the average in eq 27 is dominated by the internal chain sections with $h(s)$ given by eq 17, we expect that $(s/a)^{3/2}\bar{h}(s)$ has linear dependence on the curvilinear distance $s = ak$ between two bonds:

$$(s/a)^{3/2}\bar{h}(s) = \tilde{A} + \tilde{B}(T)(s/a) \tag{28}$$

Near the θ-temperature we may neglect the temperature dependence of $\tilde{A}$ and the function $\tilde{B}(T)$ can be approximated by the expression

$$\tilde{B}(T) = \tilde{B}_0(1 - \theta/T) \tag{29}$$

with the dimensionless parameter $\tilde{B}_0$.

In Figure 2, the numerical data for the series of temperatures are presented by different symbols and fitted by the linear dependence, eq 28, with the single value of $\tilde{A} = 0.26$, and the function $\tilde{B}(T)$ given by eq 29 with the parameter $\tilde{B}_0 = 0.15$ and the theta temperature $\theta = 2.9\epsilon/k_B$. Note that all points are well within the θ-region with the interacting parameter $|z| \ll 1$, eq 20. Thus, numerical simulations of flexible chains confirm the importance of long-range correlations in the θ-region.

2.5. Effect of Chain Flexibility. In this section we consider the effect of chain flexibility on the bond vector correlation function. Classical description of chain flexibility is given by the worm-like chain model, that predicts the exponential decay

of the bond vector correlation function, eq 1, at the persistence length $l_p = b/2$. In addition to stiffness-induced correlations, leading to the exponential decay of the orientational memory, eq 1, there are correlations in orientations of monomers that are far along the chain, but approach each other in the course of thermal fluctuations by forming temporary loops. In semiflexible chains the probability of monomeric contacts is reduced at separation s along the chain between monomers shorter than $s_* \simeq 11l_p$.[25−27] The probability of formation of a loop of length s and persistence length l_p was studied in details with the resulting approximate expression:[27]

$$J(s) = \begin{cases} \dfrac{4.7 \times 112}{(bl_p)^{3/2}} \left(\dfrac{s}{l_p}\right)^{-5} e^{-14l_p/s+0.25s/l_p} & s < s_* \\ \left(\dfrac{3}{2\pi bs}\right)^{3/2} & s > s_* \end{cases} \quad (30)$$

This probability of loop formation, $J(s)$, replaces the corresponding probability $Q(s|0)$ of a flexible chain in eq 19 for the bond vector correlation function $h(s)$. At short distances along the chain, $s < s_*$, short-range elastic interactions between bonds lead to additional exponential decay of correlations between directions of chain bonds, see eq 1. The resulting bond vector correlation function at θ-conditions, valid both at $s < s_*$ and $s > s_*$, can be represented in the following form:

$$h(s) = e^{-s/l_p}(1 - e^{-s_*/s}) + \frac{1}{a^2}\frac{2A}{3}J(s) \quad (31)$$

The step-like function $1 - e^{-s_*/s}$ assures that at short distances along the chain $s \ll s_*$ the bond vector correlation function is

$$h(s) = e^{-s/l_p} + \frac{1}{a^2}\frac{2A}{3}J(s)$$

while for longer distances along the chain the expression for flexible chains, eq 19, is restored.

In our simulations the chain stiffness is introduced through the bending potential

$$U_b(\phi) = u(1 - \cos\phi) \quad (32)$$

where ϕ is the angle between neighboring bonds i and $i + 1$, and u is the stiffness of the bending potential. The persistence length of such chains depends on u and for large $u \gg k_BT$ becomes proportional to it: $\lim_{u\to\infty}(l_p/u) = \sigma/k_BT$.

Figure 3 shows the bond vector correlation function for chains with different persistence lengths l_p at the theta temperature estimated for chains with length $L \approx 100l_p$ to be $T = \theta = 3.1\epsilon/k_B$. The persistence length l_p was determined from the initial exponential decay of $\bar{h}(s)$. Using these values of l_p we subtract the exponential decay component $e^{-s/l_p}(1 - e^{-s_*/s})$ from the bond vector correlation function $\bar{h}(s)$ and plot the difference in Figure 4.

The horizontal axis in this figure is scaled by the persistence lengths l_p, as in Figure 3, and the vertical axis is scaled by $(l_p/d)^3$, where d is the interaction radius. For the short-range LJ potential, eq 25, the interaction radius is $d = \sigma$, but it can be much larger in the case of the long-range potentials. The rescaling of the vertical axis reflects the expected dependence of the probability of two monomers separated by the distance $s \gg s_*$ along the chain to be found at the interaction radius d from each other, $d^3/(sl_p)^{3/2} = (d/l_p)^3(l_p/s)^{3/2}$. Thus, for a given value of s/l_p, the factor $(l_p/d)^3$ is expected to collapse the data for the bond vector correlation function. The theoretical expres-
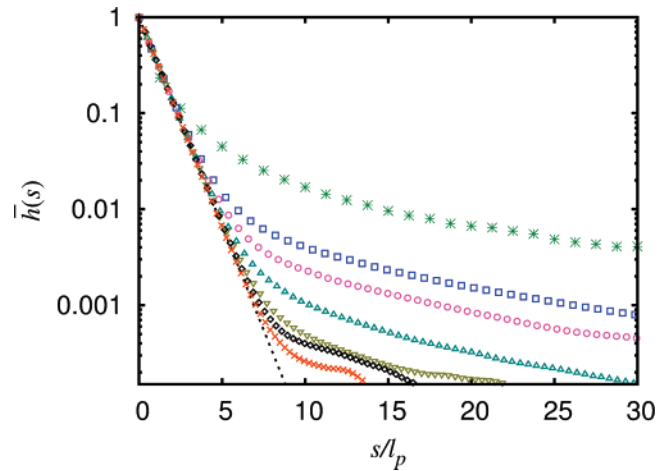

Figure 3. Averaged bond vector correlation function $\bar{h}(s)$ of polymer chains with different stiffness. Points represent the simulation results for $n = 319$ and $T = \theta = 3.1\epsilon/k_B$. Horizontal axis is scaled by the corresponding persistence length l_p, dotted line shows the exponential function e^{-s/l_p}. The symbols correspond to data for chains with different l_p (in units of σ): ($\square$) $l_p = 1.34$, ($\bigcirc$) $l_p = 1.67$, ($\triangle$) $l_p = 2.05$, ($\triangledown$) $l_p = 2.47$, ($\diamond$) $l_p = 2.91$, and ($\times$) $l_p = 3.42$; ($*$) fully flexible polymer with $l_p = 0.9\sigma$.
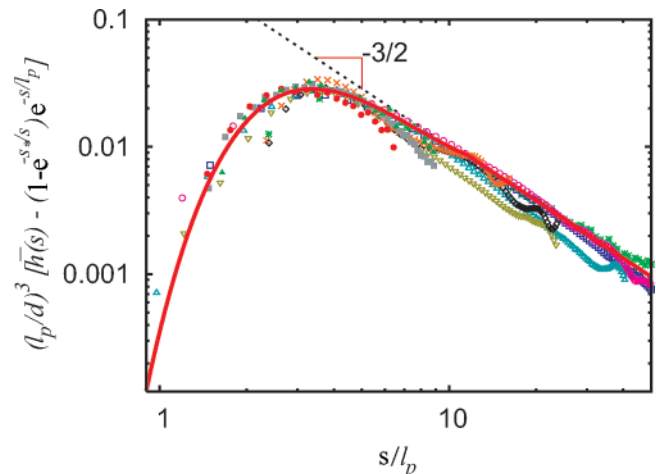

Figure 4. Residual nonexponential decay of the bond vector correlation function. Numerical data are shown by symbols: open symbols correspond to uncharged polymers with the persistent lengths l_p (in units of a): ($\square$) $l_p = 1.34$, ($\bigcirc$) $l_p = 1.67$, ($\triangle$) $l_p = 2.05$, ($\triangledown$) $l_p = 2.47$, ($\diamond$) $l_p = 2.91$, and ($\times$) $l_p = 3.42$; ($*$) fully flexible polymer with $l_p = 0.9\sigma$, closed symbols correspond to charged polymers at concentration c (in units of σ^{-3}) and the persistent length l_p (in units of a): ($\blacksquare$) $l_p = 4.74$, $c = 0.05$; ($\bullet$) $l_p = 3.42$, $c = 0.10$; ($\blacktriangle$) $l_p = 3.04$, $c = 0.15$. The solid line is the theoretical prediction for the residual nonexponential part of the bond-vector correlation function, eq 33 with $\hat{A} = 0.34$ and $s_* = 11$. The dashed line shows the power low asymptote of eq 33 for large s.

sion for the residual nonexponential part of this function derived from eq 31

$$(l_p/d)^3[h(s) - e^{-s/l_p}(1 - e^{-s_*/s})] \simeq \left(\frac{l_p}{d}\right)^3 \frac{2A}{3a^2}J(s) = \hat{A}\left(\frac{2\pi bl_p}{3}\right)^{3/2} J(s) \quad (33)$$

is shown by the solid line in Figure 4. The coefficients obtained by fitting the numerical data to eq 33 are

$$\hat{A} \equiv \left(\frac{al_p}{d^2}\right)^{3/2} \tilde{A} = \frac{2}{3}\left(\frac{3l_p}{2\pi b}\right)^{3/2}\frac{A}{a^2d^3} = 0.34 \quad (34)$$

where we used eq 18.

The nonmonotonic nature of the solid curve, eq 33, also exhibited by numerical data, is related to the reduction of the loop formation probability due to different effects. Loops with small contour length $s \lesssim s_*$ have lower probability due to the chain stiffness ($\sim e^{-14l_p/s}$), while loops, formed by long chain sections with $s \gg s_*$ have probability decreasing as $(s/l_p)^{-3/2}$. As the result of these two effects the solid curve, eq 33, reaches its maximum at $s \simeq 3.3l_p$.

The data for chains without additional bending potential (without $U_b(\phi)$, eq 32), are also shown on the same plot to illustrate the universal nature of the long-range correlations in polymers. Since the regular definition of the persistence length (see eq 1) is inapplicable for these chains, we use $l_p = 0.9\sigma$ in order to overlap the numerical data for the chain without the bending potential with the results for chains with the bending potential $U_b(\phi)$, eq 32.

In semidilute polyelectrolyte solutions electrostatic interactions are screened by charges of neighboring chains and by counterions at the distance on the order of the correlation length ξ. This correlation length $\xi \approx (f^2 a b l_B)^{-1/6} c^{-1/2}$ is calculated by scaling models as the average minimal distance between monomers of neighboring chains. Here f is the fraction of charged monomers, $l_B = e^2/k_B T$ is the Bjerrum length, c is the number density of monomers, and the solvent is θ-like for the uncharged backbone. The number of monomers in a chain section of size ξ is $g \approx (f^2 a b l_B)^{-1/2} c^{-1/2}$.[29,30] Charged polymers in semidilute solutions become flexible only at scales larger than the correlation length ξ, and have the persistence length on order of the correlation length $l_p \sim \xi$.[30]

Details of molecular dynamics simulations of semidilute polyelectrolyte solutions are given in ref 31. The results of these simulations for the bond vector correlation function are shown in Figure 4 by solid symbols, using the persistence length l_p, determined from the initial exponential decay of this function ($l_p/\xi = 1.25 \pm 0.04$, 1.32 ± 0.04, and 1.45 ± 0.04 for solutions with concentrations $c = 0.05\sigma^{-3}$, $0.10\sigma^{-3}$ and $0.15\sigma^{-3}$, respectively). Weak increase in the ratio l_p/ξ with concentration c is in agreement with the recent predictions of Dobrynin.[14] The correlation length ξ determines the characteristic scale $d = \xi$ of the interaction between chain segments. The data for polyelectrolyte solutions fall onto the same curve as the corresponding data for uncharged chains, indicating the universality of connectivity correlations.

We conclude, that for all polymers near the θ-point (with $|B| \ll A/(bs)$) the bond vector correlation function consists of two contributions — the exponential decay due to chain stiffness, and contact probability contribution, decaying as $s^{-3/2}$ (data points in Figure 4), in good agreement with the theoretical prediction, eq 33 (solid lines in Figure 4).

3. Polymer Conformations

3.1. Size of Chain Sections in the θ-Region.

Our new theory allows us to calculate the size of the chain section between bonds k and l ($k < l$) in the θ-region:

$$\langle r^2 \rangle = \left\langle \sum_{i=k}^{l} \sum_{j=k}^{l} \mathbf{a}_i \mathbf{a}_j \right\rangle = a^2 \sum_{i=k}^{l} \sum_{j=k}^{l} h(i,j) \quad (35)$$

where the bond vector correlation function $h(i,j)$ is defined in eq 10. If bonds i and j are both located far from chain ends ($i \gg j - i$ and $n - j \gg j - i$), then the bond vector correlation function, eq 12, depends only on the curvilinear distance $s = a(j - i)$ between the two bonds i and j. In this case the

expression 35 for the mean squared size of the segment can be simplified by replacing the double summation by the single sum

$$\langle r^2 \rangle = a^2(l - k) + 2a^2 \sum_{m=1}^{l-k} (l - k + 1 - m)h(am) \quad (36)$$

The first term originates from $l - k$ diagonal elements with $k = l$ of the sum in eq 35. Nondiagonal elements can be regrouped according to the separation $m = j - i$ between the two bonds i and j. Note that there are $2(l - k + 1 - m)$ identical elements of the sum in eq 35 with a given $m = j - i$. For large curvilinear distances $s = a(l - k)$ the summation over index m can be replaced by the integration over the curvilinear length $s' = am$

$$\langle r^2 \rangle = as + 2 \int_{\gamma a}^{s} (s - s')h(s') \, ds' \quad (37)$$

where γa is the lower cutoff of the integral with dimensionless parameter $\gamma \sim 1$. Substituting expression 17 for the function $h(s')$ into eq 37 and performing the integration over the variable s', we find

$$\langle r^2 \rangle \simeq bs - 8\tilde{A}a^{3/2}s^{1/2} + \frac{8}{3}\tilde{B}a^{1/2}s^{3/2} + \beta a^2 \quad (38)$$

with the Kuhn length

$$b = a(1 + 4\tilde{A}\gamma^{-1/2} - 4\tilde{B}\gamma^{1/2}) \quad (39)$$

and the dimensionless constant

$$\beta = 4\tilde{A}\gamma^{1/2} + (4/3)\tilde{B}\gamma^{3/2} \quad (40)$$

Deviations of the segment statistics from the ideal one, $\langle r^2 \rangle \sim s$, can be best visualized by plotting the ratio of the mean squared size $\langle r^2 \rangle$ to the product of the contour length and the monomer size as the function of the dimensionless variable $x = \sqrt{a/s}$. From eq 38, we find the theoretical prediction for the segment nonideality

$$\left.\frac{\langle r^2 \rangle}{as}\right|_{s=a/x^2} \simeq \frac{b}{a} - 8\tilde{A}x + \frac{8}{3}\frac{\tilde{B}}{x} + \beta x^2 \quad (41)$$

The data for $\langle r^2 \rangle/(as)$ obtained by numerical simulations at different temperatures are plotted as functions of $x = (a/s)^{1/2}$ in Figure 5.

The best fit of this set of data by the theoretical prediction, eq 41, is shown in Figure 5 by the corresponding set of lines. This fit is obtained by the following procedure. The value of the coefficient $\tilde{A} = 0.26$ is taken from the analysis of the bond vector correlation function presented in section 2.4. The temperature dependence of the coefficient $\tilde{B}(T) = \tilde{B}_0(1 - \theta/T)$ (with $\tilde{B}_0 = 0.15$ and $\theta = 2.9\epsilon/k_B$) is also taken from the same analysis. The only two adjustable parameters (b and β) were fitted separately for each temperature and their values are in excellent agreement with theoretical predictions, eqs 39 and 40, for the value of $\gamma = 0.76$.

The family of curves in Figure 5 has a shape of a trumpet and can be split into two groups. Curves of the lower group, corresponding to the negative second virial coefficient $B < 0$, exhibit pronounced maxima, that shift to higher values of x (lower values of s) with decreasing temperature. The existence of these maxima cannot be explained by classical theories and is entirely due to our correlation-induced interactions. This theoretical prediction for the locus of the maxima of the lower
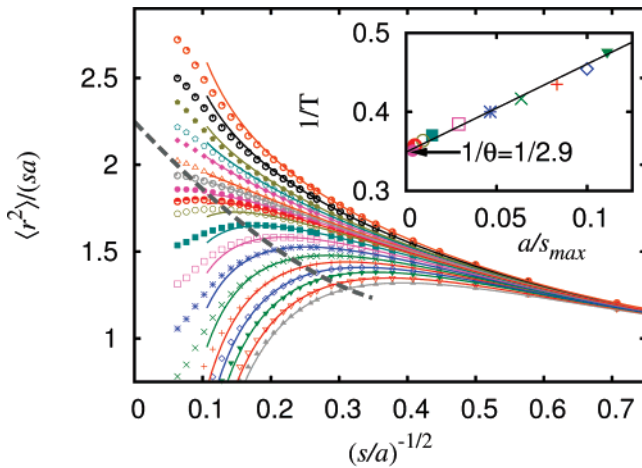
Figure 5. Dependence of the ratio of the mean squared size of a segment of the length s to as on the reciprocal square root of the number of bonds in this segment $x = (s/a)^{-1/2}$ at different temperatures. The temperatures are increasing from lower to upper curves as 1.6, 1.8, 2.0, 2.1, 2.2, 2.3, 2.4, 2.5, 2.6, 2.7, 2.75, 2.8, 2.85, 2.9, 3.0, 3.1, 3.2, 3.5, and 4.0 in units of ϵ/k_B. Lines are best fit to the numerical data by the theoretical prediction (eq 41) for $s/a \leq n/3$. The inset shows the dependence of the reciprocal temperature $1/T$ on the reciprocal number of monomers a/s_{max} of the strand at the maximum. The line in the inset corresponds to the best fit of these data to the asymptotic dependence; see eq 42.

group of curves is shown by the dashed line in Figure 5. From eq 41, the asymptotic expression for the temperature dependence of the position of the maxima is

$$s_{max} = a \frac{3\tilde{A}}{|\tilde{B}(T)|} = a \frac{3\tilde{A}}{\tilde{B}_0(\theta/T - 1)} \qquad (42)$$

The dependence $1/T$ on s_{max}^{-1} is shown in the inset of Figure 5, and in accordance with eq 42, it is well approximated by the straight line. Note that the interaction parameter $|z| \ll 1$ (see eq 20) for sections of the chain, corresponding to this maximum. These sections are much smaller than the thermal blob strands,[19] $s_{max} \ll s_{th}$, where s_{th} is the number of monomers in the thermal blob

$$s_{th} \sim \tilde{B}^{-2}(T) \sim (\theta/T - 1)^{-2} \qquad (43)$$

Curves of the second (upper) group, corresponding to the positive second virial coefficient $B > 0$, bend upward as they approach the vertical axis ($x = 0$) in Figure 5. Equation 41 predicts, that curves of this group have hyperbolic shape in the θ-region

$$\frac{\langle r^2 \rangle}{as} \simeq \frac{\tilde{B}(T)}{x} \simeq \left(\frac{s}{s_{th}} \right)^{1/2} \qquad (44)$$

where the contour length s_{th} of the thermal blob is given by eq 43. At higher temperatures in a good solvent region one expects the asymptotic behavior

$$\frac{\langle r^2 \rangle}{as} \simeq \left(\frac{s}{s_{th}} \right)^{2\nu - 1} \sim x^{2 - 4\nu} \qquad (45)$$

The only line, that asymptotically reaches the vertical axis ($x = 0$) corresponds to the θ-temperature ($B = 0$). Our theory, eq 41, predicts that at the θ-point $\langle r^2 \rangle/s$ becomes a parabolic function of $x = \sqrt{a/s}$, but the contribution of x^2 term is only important for short chain sections. We stress that the line

$\langle r^2 \rangle/s$ is not horizontal even at the θ-point, and the main deviation from the ideality is due to the linear term $\langle r^2 \rangle/s \simeq b - 8\tilde{A}a^{3/2}\sqrt{s}$. This deviation leads to s dependence of the Flory characteristic ratio as will be discussed in the following section.

3.2. Flory Characteristic Ratio. Polymer chain at the θ-condition is usually considered to be the reference state in the analysis of polymer conformations.[32−39] The dependence of the polymer size at the θ-temperature on the number n of main chain bonds is described by the characteristic Flory ratio.[42] Theoretically it is defined as the ratio of the mean-square end-to-end distance of the chain at the θ-point to the mean-square end-to-end distance of the freely jointed chain with n bonds of length a[40]

$$C_n = \frac{R^2}{a^2 n} \qquad (46)$$

Experimentally, it is determined as the ratio of the mean-square radius of gyration of the chain at the θ-point to the mean-square radius of gyration of the freely jointed chain of the mass M

$$C_n = \frac{6R_g^2}{a^2(M/M_0)} \qquad (47)$$

where M_0 is the molar mass per bond.

Classical chain models predict that the characteristic ratio quickly approaches its asymptotic value $C_\infty = \lim_{n \to \infty} C_n$ with increasing n, as $C_\infty - C_n \sim n^{-1}$.[41,42] Long range correlations between bond vectors of the chain described in the present paper lead to a much weaker dependence, $C_\infty - C_n \sim n^{-1/2}$.

The mean-square radius of gyration of the chain at the θ-point can be derived by analogy with eq 38:

$$R_g^2 \simeq \frac{abn}{6} - \frac{31}{12}\tilde{A}a^2\sqrt{n} + \frac{\beta}{2}a^2 \qquad (48)$$

where $b = 2l_p + 4a\tilde{A}\gamma^{-1/2}$ and $\beta = 4\tilde{A}\gamma^{1/2}$, as defined in eq 40 with $\tilde{B} = 0$. From eq 48 we obtain the expression for the characteristic ratio of long chains (ignoring the last term in this equation for $n \gg 1$) which is a linear function of $n^{-1/2} \sim M^{-1/2}$

$$C_\infty - C_n \simeq \frac{31}{2}\tilde{A}n^{-1/2} \qquad (49)$$

with asymptotic value of the characteristic ratio $C_\infty = b/a$.

The comparison of our prediction for the molecular weight dependence of the characteristic Flory ratio C_n with experimental data for polystyrene in a θ-solution[43] is shown in Figure 6. We plot the characteristic ratio C_n as the function of the reciprocal square root number of main chain bonds. As can be seen from the inset in Figure 6, the dependence of C_n on $n^{-1/2}$ is linear, as expected from eq 49 and can be fitted by $C_n = 11.9 - 30.2n^{-1/2}$. The plot shown in the inset is the best way of accurately obtaining the limiting value of the characteristic ratio C_∞ ($C_\infty = 11.9$ for polystyrene in cyclohexane). Similar $n^{-1/2}$ dependence has been also obtained in ref 20 for the inner chain segments using the self-consistent mean-field approach.

4. Conclusions

In this paper, we introduced a new type of interaction between monomers, which has not been taken into account in previous studies. This effective interaction is due to the finite range of monomeric potential and the chain connectivity. The new effect does not exist in models where chain elasticity is balanced by the excluded volume interactions of unconnected monomers, as in the Flory theory. The new connectivity-induced interaction
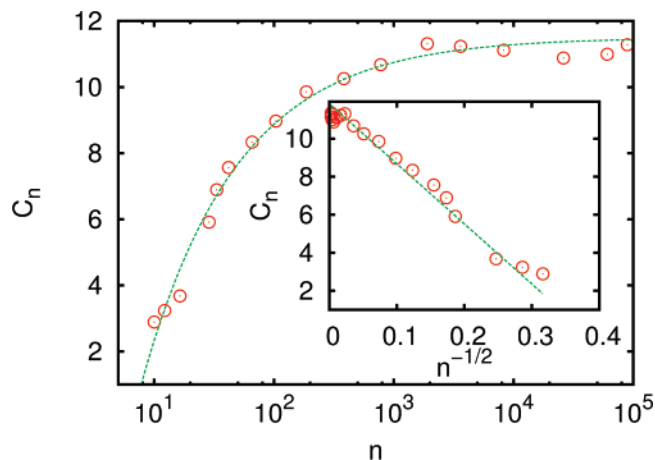
Figure 6. Flory characteristic ratio C_n for polystyrene in cyclohexane at 34.5 °C (θ-solution)[43] as the function of the number $n = M/M_0$ of main chain bonds. For polystyrene the average bond length $a \approx 1.54$Å and its mass per bond is $M_0 = 52$ g/mol. Inset: the Flory characteristic ratio C_n as the function of the reciprocal square root number of main chain bonds. Straight line is the best fit of the data by eq 49.

is also absent in the standard models with δ-function interaction potential that neglects the spatial separation of attractive and repulsive parts of monomeric interactions. Thus, there are two necessary conditions for the existence of the new connectivity-induced correlation effect, proposed in the present paper: monomer connectivity along the chain and nonzero range of interaction potential. Our analysis provides a unified description of the nonideality of polymer chains in dilute θ-solutions, melts and semidilute solutions. We focus on the change of the effective interaction between two monomers caused by the entropic elasticity of the loop formed when these monomers are in contact with each other.

This effect leads to deviations from ideality for polymers in a θ-region, such as long-range power-law correlations between directions of chain bonds $\mathbf{a}_i$ and $\mathbf{a}_{i+k}$, separated by k monomers

$$\langle \mathbf{a}_i \mathbf{a}_{i+k} \rangle \sim \begin{cases} -k^{-1/2} & k^{-1} \ll 1 - T/\theta \ll k^{-1/2} \\ k^{-3/2} & |T/\theta - 1| \ll k^{-1} \\ k^{-1/2} & k^{-1} \ll T/\theta - 1 \ll k^{-1/2} \\ k^{2\nu-2} & k^{-1/2} \ll T/\theta - 1 \end{cases} \quad (50)$$

The first and third dependencies are caused by two-body attraction and repulsion, respectively, in the θ-region. The second dependence is due to our new effective interaction at temperatures T close to the θ-temperature. The fourth relation is the result of excluded volume interactions away from the θ-point.[44]

These correlations lead to unexpected dependence of the ratio of the mean-square size $\langle r^2 \rangle$ of the chain section to its ideal size $\langle r^2 \rangle_{id} = abk$ on the number of monomers k in this section

$$\frac{\langle r^2 \rangle}{\langle r^2 \rangle_{id}} - 1 \sim \begin{cases} -k^{1/2} & k^{-1} \ll 1 - T/\theta \ll k^{-1/2} \\ -k^{-1/2} & |T/\theta - 1| \ll k^{-1} \\ k^{1/2} & k^{-1} \ll T/\theta - 1 \ll k^{-1/2} \\ k^{2\nu-1} & k^{-1/2} \ll T/\theta \ll -1 \end{cases} \quad (51)$$

The best way to visualize these dependencies is to plot the above ratio, eq 51, as the function of $x = k^{-1/2}$; see Figure 5. The only curve, that asymptotically reaches the vertical axis $x = 0$ corresponds to the θ-point. The negative slope of this line is determined by the strength of our new effective

interactions. The group of curves, corresponding to positive second virial coefficients bend upward away from this line. Curves, corresponding to negative second virial coefficients bend downward away from this line and have pronounced maxima due to the balance of new effective interactions and two body attraction. These maxima occur well in the θ-region with the energy of the two body attraction much less than the thermal energy $k_B T$. We also predict similar behavior for the n dependence of the characteristic Flory ratio C_n, (see eq 49 and the inset in Figure 6 for this behavior at $T = \theta$). The characteristic ratio C_n should have a maximum in the θ-region at temperatures $T < \theta$.

We demonstrate, that the effect of newly discovered correlation-induced interactions dominates over classical logarithmic corrections due to tricritical fluctuations in a wide range of chain sizes, $n \lesssim n_{ren} \simeq 10^4$, and over the significant temperature window around the θ-point (see, for example, Figure 2). For longer chains tricritical fluctuations become important for sections containing $k > n_{ren}$ monomers. Logarithmic corrections to the bond vector correlation function become important for bonds separated by such very long sections, for which we get

$$\langle \mathbf{a}_i \mathbf{a}_{i+k} \rangle \sim \begin{cases} k^{-3/2} w^{-4/11} & |T/\theta - 1| \ll k^{-1} w^{8/33} \\ k^{-1/2} w^{-4/33} & k^{-1} w^{8/33} \ll |T/\theta - 1| \ll k^{-1/2} \end{cases} \quad (52)$$

and the function $w = w(ak)$ is defined in eq 23.

Although this paper focuses on polymer properties in the θ-region, the effect of new effective interactions on chain conformations is also important outside the θ-region, as will be shown in the forthcoming publication.[45] These effective interactions are important not only for dilute solutions near the θ-point, but also in melts and semidilute solutions, both in good and θ-solvents.[18] In the case of semidilute solutions, this effective interactions become significant on length scales larger than the correlation length ξ.

Note that since these interactions are due to the chain connectivity, they exist exclusively between sections of the same chain, rather than sections of different chains. These effective interactions are due to small correlations in relative positions of segments located far along the contour of the chain, as they meet each other in the process of thermal fluctuations. The probability of such encounters between chain sections is significantly reduced in semiflexible chains, decreasing the effect of these interactions.

Predictions of our theory can be tested by extensive computer simulations and systematic experiments. Our theory provides a new basis for the analysis of polymer properties near the θ-point. In particular, the systematic investigation of the Flory characteristic ratio at the θ-region provides a direct measurement of the strength of the new interactions for different classes of polymers. Results of these experiments can be directly compared with measurements of the bond vector correlation function of the same polymer as well as with corresponding computer simulations and will provide the stringent test of our theory.

Appendix A. Bond Vector Correlations for a Fixed End-to-End Vector

Consider a Gaussian chain with n bonds of the average bond length a, contour length $L = an$, and fixed end-to-end vector $\mathbf{r}$.

The bond vector correlation function $H(L|r)$ for fixed r can be found by averaging the square of both sides of eq 3 over the fluctuations of bond vectors $\{\mathbf{a}_i\}$:

$$r^2 = n\langle \mathbf{a}_i^2 \rangle_r + n(n-1)a^2 H(L|r) \tag{53}$$

The mean square length of the bond at fixed end-to-end vector $\mathbf{r}$

$$\langle \mathbf{a}_i^2 \rangle_r = \langle \mathbf{a}_i \rangle_r^2 + \langle \delta \mathbf{a}_i^2 \rangle_r \tag{54}$$

depends on the length of this end-to-end vector and may differ from a^2 of free chain. Averaging eq 3 over the fluctuations of bond vectors $\mathbf{a}_i$ for a given vector $\mathbf{r}$ we find

$$\langle \mathbf{a}_i \rangle_r = \mathbf{r}/n \tag{55}$$

In contrast to the average, $\langle \mathbf{a}_i \rangle_r$, the amplitude of fluctuations of the bond vector $\delta \mathbf{a}_i = \mathbf{a}_i - \langle \mathbf{a}_i \rangle_r$ of a Gaussian chain does not depend on $\mathbf{r}$. Fixing the chain ends at a constant distance decreases the number of degrees of freedom of this chain from n to $n-1$, and thus reduces the average bond fluctuations by the factor of $(n-1)/n$:

$$\langle \delta \mathbf{a}_i^2 \rangle_r = \frac{n-1}{n} a^2 \tag{56}$$

Substituting eqs 56 and 55 into 54, and plugging in the resulting expression for $\langle \mathbf{a}_i^2 \rangle_r$ into eq 53 we get

$$H(L|r) = \frac{r^2}{a^2 n^2} - \frac{1}{n} \tag{57}$$

Using the expression for the contour length $L = an$ we obtain the final expression (eq 5) for the bond vector correlation function, $\langle \mathbf{a}_i \mathbf{a}_j \rangle_r$, at fixed end-to-end vector $\mathbf{r}$.

Appendix B. Average Bond Vector Correlation Function of a Telechelic Chain

To calculate the bond vector correlation function $H(L)$, defined in eq 4, we average $H(L|r)$ (eq 5 or 5) over end-to-end distances r with the probability $\mathscr{P}(L|r)$ of chain conformation with a given end-to-end vector $\mathbf{r}$:

$$H(L) \equiv \int \mathscr{P}(L|r) H(L|r) \, \mathrm{d}^3 r \tag{58}$$

Here

$$\mathscr{P}(L|r) = \frac{Q(L|r)\, e^{-U(r)/k_B T}}{\int Q(L|r')\, e^{-U(r')/k_B T}\, \mathrm{d}^3 r'} \tag{59}$$

$Q(L|r)$ is the probability distribution to find ends of a Gaussian chain at a given distance r from each other

$$Q(L|r) = \left(\frac{3}{2\pi bL}\right)^{3/2} \exp\left(-\frac{3r^2}{2bL}\right) \tag{60}$$

$e^{-U(r)/T}$ is the corresponding Boltzmann weight, and L is the contour length of the polymer. Substituting eq 60 into 59, and replacing the Boltzmann weight $e^{-U/k_B T}$ by unity plus the Mayer function $(1 + f(\mathbf{r})$, see eq 8), we obtain

$$H(L) = \frac{\int H(L|r)Q(L|r)\, \mathrm{d}^3 r + \int H(L|r)Q(L|r)f(r)\, \mathrm{d}^3 r}{\int Q(L|r)\, \mathrm{d}^3 r + \int Q(L|r)f(r)\, \mathrm{d}^3 r}$$

$$= \frac{\int H(L|r)Q(L|r)f(r)\, \mathrm{d}^3 r}{1 + \int Q(L|r)f(r)\, \mathrm{d}^3 r} \tag{61}$$

Since the Mayer function $f(r)$ vanishes at large r, the main contribution to this function comes from loop conformations with chain ends spatially close to each other, $r \ll (bL)^{1/2}$. Substituting the expansion of the functions $Q(L|r)$ in eq 60 in powers of r^2/L into eq 61, we obtain

$$H(L) =$$

$$\left(\frac{3}{2\pi bL}\right)^{3/2} \frac{\int H(L|r)f(r)\, \mathrm{d}^3 r - \int H(L|r)\frac{3r^2}{2bL} f(r)\, \mathrm{d}^3 r + \dots}{1 + \dots} \tag{62}$$

Expanding this result in powers of $1/L$ and keeping only leading terms in this expansion, one gets eq 6, in which the Kuhn length b is assumed to be equal to the monomer size a.

Appendix C. Renormalization Group in the Tricritical Region

In this appendix we present the results of the renormalization group (RG), the goal of which is to take into account the effect of many-body interactions between monomers on correlations between bonds and on the chain size. These calculations generalize the classical RG calculations of Duplantier[12] in order to include the nonlocality of the monomeric potential. The main idea of the real space RG is to calculate the effective interactions between larger sections of the chain from the corresponding interactions of its smaller sections.

We start from monomers of size a with the second virial coefficient B, eq 7, third virial coefficient C, and nonlocal virial coefficient A, eq 9, and define the dimensionless interaction parameters

$$u_0 = \frac{B}{(2\pi)^{3/2} a^3}, \quad y_0 = \frac{C}{(2\pi)^3 a^6}, \quad t_0 = \frac{A}{a^5} \tag{63}$$

At the first stage of RG we calculate the corresponding interaction coefficients, B_1^{sec}, C_1^{sec}, and A_1^{sec} between chain sections consisting of g monomers. The dimensionless interaction parameters are defined by dividing these interaction coefficients by the corresponding powers of the Gaussian size of these sections, $ag^{1/2}$. The same procedure is repeated for the second, third, ..., and ith step of RG with the resulting interaction parameters

$$u_i = \frac{B_i^{sec}}{(2\pi)^{3/2}(aS_i^{1/2})^3} = \frac{B_i}{(2\pi)^{3/2} a^3}$$

$$y_i = \frac{C_i^{sec}}{(2\pi)^3 (aS_i^{1/2})^6} = \frac{C_i}{(2\pi)^3 a^6}$$

$$t_i = \frac{A_i^{sec}}{(aS_i^{1/2})^5} = \frac{A_i}{a^5} \tag{64}$$

where $S_i = g^i$ is the number of monomers in the interacting section at ith step of RG, and $B_i = B_i^{sec} S_i^{-3/2}$, $C_i = C_i^{sec} S_i^{-3}$, and

$A_i = A_i^{sec} S_i^{-5/2}$ are effective monomeric interaction coefficients. Below we find the recurrence relation between these interaction coefficients at the consecutive steps of RG.

The starting point of our consideration is the effective Hamiltonian of the chain

$$\frac{H}{k_B T} = \frac{3}{2a} \int \left(\frac{d\mathbf{r}}{ds'}\right)^2 ds' -$$
$$\frac{1}{2} \int\int d^3r \, d^3r' \, f(\mathbf{r} - \mathbf{r}')\rho(\mathbf{r})\rho(\mathbf{r}') + \frac{C}{6} \int d^3r \, \rho^3(\mathbf{r}) \quad (65)$$

where $\mathbf{r}(s')$ is the position vector of the monomer with curvilinear coordinate s' and $\rho(\mathbf{r})$ is the monomeric density

$$\rho(\mathbf{r}) = a^{-1} \int \delta[\mathbf{r} - \mathbf{r}(s')] \, ds' \quad (66)$$

In the case of local pair interactions, the Mayer function can be approximated by the δ-function, $f(\mathbf{r} - \mathbf{r}') = -B\delta(\mathbf{r} - \mathbf{r}')$, and the two-body interaction term of the Hamiltonian in eq 65 takes the standard form

$$\frac{B}{6} \int d^3r \, \rho^2(\mathbf{r}) = \frac{B}{2a^2} \int\int ds' \, ds'' \, \delta[\mathbf{r}(s') - \mathbf{r}(s'')]$$

In this paper, we consider nonlocal interactions, for which the Mayer function cannot be represented as a simple δ-function. Keeping the pair interactions between monomers in a more general nonlocal form and substituting expression 66 for the monomeric density into eq 65, we obtain the generalization of the Edwards Hamiltonian[46]

$$\frac{H}{k_B T} = \frac{3}{2a} \int \left(\frac{d\mathbf{r}}{ds'}\right)^2 ds' - \frac{1}{2a^2} \int\int ds' \, ds'' \, f[\mathbf{r}(s') - \mathbf{r}(s'')] +$$
$$\frac{C}{6a^3} \int\int\int ds' \, ds'' \, ds''' \, \delta[\mathbf{r}(s') - \mathbf{r}(s'')]\delta[\mathbf{r}(s') - \mathbf{r}(s''')]$$
$$(67)$$

The main idea is that at the ith step of RG the Hamiltonian of the chain has the same form, but with renormalized coefficient C_i and the renormalized Mayer function f_i. Integrals in eq 67 at each step of RG are replaced by the sum of integrals over sections of length S_i of the chain

$$\int_0^{an} ds_{i-1} \dots = \sum_{k=1}^{n/S_i} \int_{aS_i(k-1)}^{aS_ik} ds_i \dots \quad (68)$$

The calculation involves averaging over the conformations of these sections. The result of this averaging is the new effective renormalized parameter C_i and the Mayer function f_i.

Three body interactions give the dominant contribution to the renormalization of the third virial coefficient in the tricritical region near the θ-point. As shown in ref 12, the effective third virial coefficient C_i at step i is related to this coefficient C_{i-1} at step $i - 1$ as

$$C_i = C_{i-1} - \frac{11}{2\pi^2 a^3} C_{i-1}^2 \ln g \quad (69)$$

The number S_i of monomers in interacting sections increases by the factor of g at each step of RG, $S_i = S_{i-1}g$. Using the relation $\ln g = \ln S_i - \ln S_{i-1}$, eq 69 can be rewritten as

$$\frac{C_i - C_{i-1}}{\ln S_i - \ln S_{i-1}} = -\frac{11}{2\pi^2 a^3} C_{i-1}^2 \quad (70)$$

Substituting $C_i = y_i a^6 (2\pi)^3$ from eq 64 into eq 70, we obtain

$$\frac{y_i - y_{i-1}}{\ln S_i - \ln S_{i-1}} = -44\pi y_i^2 \quad (71)$$

These equations can be rewritten in the continuous differential form (keeping $g \gg 1$)

$$\frac{dy}{d(\ln S)} = -44\pi y^2 \quad (72)$$

A similar procedure leads to RG equations for the dimensionless second virial coefficient u and the dimensionless nonlocal virial coefficient t, see eq 64, where interaction coefficients A_i and B_i are obtained by integrals (eqs 7 and 9) of the renormalized Mayer function $f_i(\mathbf{r})$ at the ith step of RG:

$$\frac{du}{d \ln S} = -16\pi u y, \quad \frac{dt}{d \ln S} = -\frac{16\pi}{3} t y \quad (73)$$

The solution of the system of eqs 72 and 73 can be obtained by separation of variables with the result

$$y = y_0/w, \quad u = u_0 w^{-4/11}, \quad t = t_0 w^{-4/33} \quad (74)$$

$$w = 1 + 44\pi y_0 \ln (S/a) \quad (75)$$

where y_0, u_0, and t_0 are bare values of dimensionless interaction parameters, eq 63. Expressions for y and u reproduce the result of Duplantier,[12] while t describes the renormalization of the parameter A due to tricritical fluctuations.

Appendix D. Table of Notations

symbol	meaning
a	average length of the bond vector
$\mathbf{a}_i$	ith bond vector, $\langle \mathbf{a}_i \rangle = a$
A	second moment of the Mayer f-function, eq 9
$\tilde{A}, \hat{A}$	dimensionless A, eqs 18 and 34
b	Kuhn segment length
B	second virial coefficient, eq 7
$\tilde{B}$	dimensionless B, eq 18
c	monomeric concentration
C	third virial coefficient
C_n	Flory characteristic ratio for chain of n bonds eq 47
C_∞	asymptotic value of C_n for infinite chain, $C_\infty = b/a$
d	interaction radius
f	fraction of charged monomers of the chain
$f(r)$	Mayer f-function, eq 8
g	number of monomers per correlation blob
$g_{1/2}(i, j), g_{3/2}(i, j)$	contributions to $h(i, j)$ with coefficients B and A, respectively, eq 13
$h (i, j), h(s)$	bond vector correlation function for interacting chain, eqs 10 and 14
$H(L), H(L\|r)$	bond vector correlation functions for telechelic polymer, eqs 4 and 5
$J(s)$	probability of loop formation for the semiflexible chain of length s, eqs 30
k_B	Boltzmann constant
L	polymer contour length, $L = an$
l_p	persistence length, eq 1
M	polymer molar mass
M_0	molar mass per bond
n	number of bonds in macromolecule

$Q(L\|r)$	probability to find ends of Gaussian chain of length L at a distance r, eq 60
r	distance between monomers
r_c	Lennard-Jones cutoff distance, eq 25
R^2	mean-square end-to-end distance of a chain
R_0	FENE bond extension limit, eq 26
R_g^2	mean-square gyration radius of a chain
s	contour length
T	absolute temperature
u	stiffness of the bending potential, eq 32
$U(r), U_{FENE}(r)$	monomeric interaction potentials
$U_b(\phi)$	bending potential, eq 32
x	dimensionless variable $x = \sqrt{a/s}$
$w(s)$	renormalization factor due to tricritical fluctuations, eq 23
z	interaction parameter, eq 20
β	dimensionless constant, eq 40
γ	dimensionless coefficient for lower cutoff, eq 37
ϵ	amplitude of the Lennard-Jones interaction potential, eq 25
ξ	correlation length
σ	molecular dynamics length unit
τ_R	polymer relaxation time
ϕ	bond angle, eq 32

References and Notes

(1) Edwards, S. F. *Proc. Phys. Soc.* **1964**, *85*, 613−624.
(2) Moore, M. A. *J. Phys. A* **1977**, *10*, 305−314.
(3) Flory, J. P. *J. Chem. Phys.* **1949**, *17*, 303−313.
(4) Ptitsyn, O. B.; Eizner, Y. E. *Biofizika* **1965**, *10*, 3−6.
(5) de Gennes, P. G. *J. Phys. (Paris) Lett.* **1975**, *36*, L55.
(6) Lifshitz, I. M.; Grosberg, A. Y.; Khokhlov, A. R. *Rev. Mod. Phys.* **1978**, *50*, 683−713.
(7) Birshtein, T. M.; Pryamitsyn, V. *Vysokomol. Soedin.* **1987**, *29*, 1858−1864.
(8) Yamakawa, H. *Modern Theory of Polymer Solutions*; Harpers Chemistry Series; Harper and Row: New York, 1971.
(9) des Cloizeaux, J.; Jannink, G. *Polymers in Solution*; Clarendon Press: Oxford, U.K., 1990.
(10) Kholodenko, A. L.; Freed, K. F. *J. Chem. Phys.* **1984**, *80*, 900−924.
(11) Cherayil, B. J.; Douglas, J. F.; Freed, K. F. *J. Chem. Phys.* **1985**, *8*, 5293−5310.
(12) Duplantier, B. *J. Chem. Phys.* **1987**, *86*, 4233−4244.
(13) Brulet, A.; Boue, F.; Cotton, J. P. *J. Phys. (Paris) II* **1996**, *6*, 885−891.
(14) Dobrynin, A. V. *Macromolecules* **2005**, *38*, 9304−9314.
(15) Lecommandoux, S.; Checot, F.; Borsali, R.; Schappacher, M.; Deffieux, A.; Brulet, A.; Cotton, J. P. *Macromolecules* **2002**, *35*, 8878−8881.
(16) Rivetti, C.; Walker, C.; Bustamante, C. *J. Mol. Biol.* **1998**, *280*, 41−59.
(17) Sheiko, S. S.; Sun, F. C.; Randall, A.; Shirvanyants, D.; Rubinstein, M.; Lee, H.-i.; Matyjaszewski, K. *Nature (London)* **2006**, *440*, 191−194.
(18) Wittmer, J. P.; Meyer, H.; Baschnagel, J.; Johner, A.; Obukhov, S.; Mattioni, L.; Muller, M.; Semenov, A. N. *Phys. Rev. Lett.* **2004**, *93*, 147801.
(19) de Gennes, P. G. *Scaling concepts in polymer physics*; Cornell University: Ithaca, NY, 1979.
(20) Allegra, G. *Macromolecules* **1983**, *16*, 555−559.
(21) Khokhlov, A. R. *Polymer* **1978**, *19*, 1387−1396.
(22) Zimm, B. H.; Stockmayer, W. H.; Fixman, M. *J. Chem. Phys.* **1953**, *21*, 1716−1722.
(23) Yamakawa, H.; Aoki, A.; Tanaka, G. *J. Chem. Phys.* **1966**, *45*, 1938−1941.
(24) Withers, I. M.; Dobrynin, A. V.; Berkowitz, M. L.; Rubinstein, M. *J. Chem. Phys.* **2003**, *118*, 4721−4731.
(25) Shimada, J.; Yamakawa, H. *Macromolecules* **1984**, *17*, 689−698.
(26) Dua, A.; Cherayil, B. J. *J. Chem. Phys.* **2002**, *117*, 7765−7773.
(27) Allemand, J.-F.; Cocco, S.; Douarche, N.; Lia, G. *Eur. Phys. J. E* **2006**, *19*, 293−202.
(28) Landau, L.; Lifshitz, E. *Theory of elasticity*, 3rd English ed., Pergamon Press: Oxford, U.K., and New York: 1986.
(29) Odijk, T. *Macromolecules* **1979**, *12*, 688−693.
(30) Dobrynin, A. V.; Colby, R. H.; Rubinstein, M. *Macromolecules* **1995**, *28*, 1859−1871.
(31) Liao, Q.; Dobrynin, A. V.; Rubinstein, M. *Macromolecules* **2003**, *36*, 3386−3398.
(32) Webman, I.; Lebowitz, J. L.; Kalos, M. H. *Macromolecules* **1981**, *14*, 1495−1501.
(33) Kremer, K.; Baumgartner, A.; Binder, K. *J. Phys. A* **1982**, *15*, 2879−2897.
(34) Meirovitch, H.; Lim, H. A. *J. Chem. Phys.* **1989**, *91*, 2544−2554.
(35) Meirovitch, H.; Lim, H. A. *J. Chem. Phys.* **1990**, *92*, 5144−5154.
(36) Yuan, X.-F.; Masters, A. J. *J. Chem. Phys.* **1991**, *94*, 6908−6919.
(37) Rey, A.; Freire, J. J.; Bishop, M.; Clarke, J. H. R. *Macromolecules* **1992**, *25*, 1311−1315.
(38) Rubio, A. M.; Freire, J. J.; Clarke, J. H. R.; Yong, C. W.; Bishop, M. *J. Chem. Phys.* **1995**, *102*, 2277−2281.
(39) Wittkop, M.; Kreitmeier, S.; Goritz, D. *J. Chem. Phys.* **1996**, *104*, 3373−3385.
(40) Rubinstein, M.; Colby, R. H. *Polymer physics*; Oxford University Press: New York, 2003.
(41) Mattice, W. L.; Helfer, C. A.; Sokolov, A. P. *Macromolecules* **2003**, *36*, 9924−9928.
(42) Flory, J. P. *Statistical mechanics of Chain Molecules*; Interscience: New York, 1969.
(43) Konishi, T.; Yoshizaki, T.; Saito, T.; Einaga, Y.; Yamakawa, H. *Macromolecules* **1990**, *23*, 290−297.
(44) Schäfer, L.; Ostendorf, A.; Hager, J. *J. Phys. A* **1999**, *32*, 7875−7899.
(45) Withers, I. M.; Panyukov, S. V.; Shirvanyants, D.; Dobrynin, A. V.; Rubinstein, M. To be published.
(46) Doi M.; Edwards, S. F. *The Theory of Polymer Dynamics*; Clarendon Press: Oxford, U.K., 1986.